Modeling for the Performance Analysis of a Tubular SOFC/MGT Hybrid Power System

T. W. Song †, J. L. Sohn*, J. H. Kim**, T. S. Kim***, S. T. Ro*, and K. Suzuki****

원통형 고체산화물 연료전지와 마이크로 가스터빈 하이브리드 시스템의 성능해석을 위한 모델링

송 태원(서울대 원), 손 정락(서울대), 김 재환(항우연), 김 동섭(인하대), 노 승탁(서울대)
, K. Suzuki(Shibaura Inst. of Tech., Japan)

Key Words : Internal reformer, Hybrid system, MGT (Micro Gas Turbine), Tubular SOFC (Solid Oxide Fuel Cell)

Abstract

Performance of a solid oxide fuel cell (SOFC) can be enhanced by converting thermal energy of its high temperature exhaust gas to mechanical power using a micro gas turbine (MGT). A MGT plays also an important role to pressurize and warm up inlet gas streams of the SOFC. In this study, the influence of performance characteristics of the tubular SOFC on the hybrid power system is discussed. For this purpose, detailed heat and mass transfer with reforming and electrochemical reactions in the SOFC are mathematically modeled, and their results are reflected to the performance analysis. The analysis target is 220kWe SOFC/MGT hybrid system based on the tubular SOFC developed by Siemens-Westinghouse. Special attention is paid to the ohmic losses in the tubular SOFC counting not only current flow in radial direction, but also current flow in circumferential direction through the anode and cathode.

Nomenclature

A	activation area	[m^2]
F_{i-j}	shape factor between solid walls of i and j	
h	convective heat transfer coefficient	[kW/m^2-K]
$\bar{h}(T)$	molar specific enthalpy at T	[kJ/kmol]
j	current density	[A/m^2]
k_s	thermal conductivity	[kW/m-K]
LHV	lower heating value	[kJ/kg]
$\dot{n}$	molar flow rate	[kmol/s]
$\dot{Q}$	heat transfer rate	[kW]
T	temperature	[°C or K]
V	voltage	[V]
$\dot{W}$	power	[kW]
Δx	length of control volume	[m]

Greek

η	efficiency

Subscript

0	standard state of each condition
a	air gas
c	tri-layer in fuel cell
$cond$	conduction
$conv$	convection
f	fuel gas
FC	fuel cell
fp	fuel feed plates
ft	air feed tube
GT	gas turbine
m	arithmetic mean value
oc	open-circuit
rad	radiation
rw	reformer wall
SYS	hybrid system
x	species of chemical component

† School of Mech. and Aero Eng., Seoul Nat'l Univ.
E-mail : singlee@ieel.snu.ac.kr
TEL : (02)880-7119 FAX : (02)883-0179
* School of Mech. and Aero Eng., Seoul Nat'l Univ.
** Turbomachinery branch, Korea Aerospace Research Institute
*** Dept. of Mech. Eng., Inha Univ.
**** Dept. of Machinery and control system, Shibaura Inst. of Tech., Japan

1. Introduction

Theoretical feasibilities of the SOFC/MGT hybrid power system were investigated by multiple research groups since 1990's. Among them, Harvey and Richter [1], who proposed a hybrid thermodynamic cycle combining gas turbine and fuel cell, were pioneers in this field. In the process of technical evolution of the fuel cell / gas turbine hybrid power system, both SOFC [2] and MCFC (Molten Carbonate Fuel Cell) [3] were considered as possible candidates for the fuel cell. However, recent studies are focused on SOFCs because of its advantage of higher thermal efficiency than MCFCs [4]. After Siemens-Westinghouse successfully demonstrated a 100kW class SOFC-based cogeneration power system

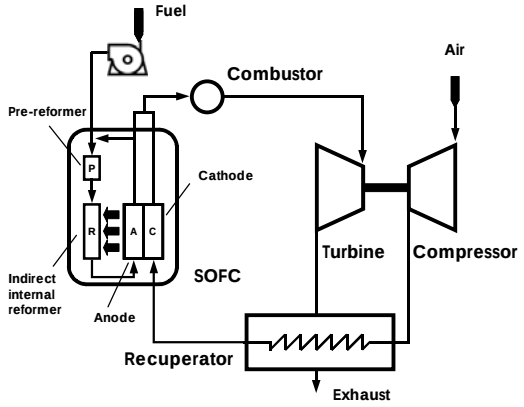

Fig. 1 Schematic diagram of SOFC/MGT hybrid power system

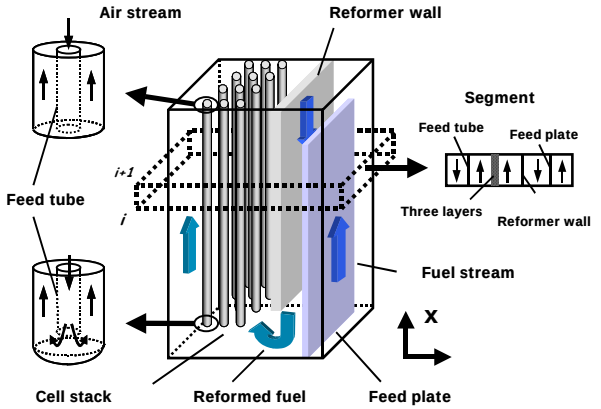

Fig. 2 Schematic diagram for quasi-2D model in the IIR-SOFC

in 2001 using their commercial tubular SOFC, they initiated to develop 220kW class SOFC/MGT hybrid power system [5,6].

In spite of the appearance of many innovative cycles for the SOFC/MGT hybrid power system, its universal configuration is not yet fully established. Studies to develop new system configurations are still under progress. Performance analysis of the hybrid system using mathematical models is an essential tool to investigate performance and operating characteristics of various configurations. Mathematical thermodynamic models of the SOFC/MGT hybrid power system have been developed by many research groups. Among them, Massardo and Lubelli [4] investigated characteristics of the design point performance of the internal reforming SOFC/MGT hybrid power system. Kim and Suzuki [7] also conducted similar study with different mathematical models.

In the present study, a quasi-2D model of the SOFC is proposed to improve the accuracy of the performance analysis of the SOFC/MGT hybrid power system. The analysis target is 220kWe SOFC/MGT hybrid system based on the tubular SOFC developed by Siemens-Westinghouse. Special attention is paid to the ohmic losses in the tubular SOFC counting not only current flow in radial direction, but also current flow in circumferential direction through the anode and cathode.

2. System configurations

A schematic diagram of the SOFC/MGT hybrid power system to be investigated in this study is shown in Fig. 1, which is the same as that of Siemens-Westinghouse [5,6]. Compressed fuel (methane) is fed to reformers, and supplied to the anode side of the SOFC after reforming reactions. Air supplied from the ambient is compressed by the compressor driven by the turbine, and heated in the recuperator by the hot gas stream of turbine exhaust. High temperature and high pressure air then enters the cathode side of the SOFC, and is electrochemically reacted at the electrode/electrolyte interfaces with fuel (hydrogen and carbon monoxide) supplied from the anode side of the SOFC producing electric power. Non-reacted fuel in the exhaust gas of the SOFC is burnt in the combustor and expands in the turbine. Part of shaft power produced by the turbine is converted to electric power by electric generator.

Fuel cell stacks in Fig. 2 are composed of bundles of multiple tubular SOFCs, which are tubes with a length of 150 cm and 2.2 cm as a diameter [8,9]. Each SOFC bundle is composed by 24 tubular SOFCs as 3 rows of 8 serially connected ones. Each tubular SOFC is sealed at one end. Tube wall is composed of tri-layer; cathode (inner wall), electrolyte, and anode (outer wall).

Supplied fuel is partially reformed in the pre-reformer whose role is to reduce reforming load of internal reforming processes. Partially reformed fuel at the exit of pre-reformer enters the indirect internal reformer (IIR) guided by fuel feed plates and reformed again by the aid of heat supplied from the SOFC through reformer walls. Reformed fuel entering the SOFC stacks flows along outside of the tube from the sealed bottom towards the open end.

Air is fed through a thin air feed tube located centrally inside each tubular SOFC and, then, flows back up to the open end of the SOFC.

Fuel and air streams along the longitudinal direction of the tubular SOFC participate into electrochemical reactions and produce steam with generation of electric power. Temperatures of both streams are raised due to the exothermic electrochemical reaction. Some portion of effluent in depleted fuel plenum is recirculated to the inlet of pre-reformer supplying necessary steam and heat for the reforming reaction. The amount of recirculated steam, denoted by the steam-carbon ratio, is an important design parameter related to the system performance.

3. Mathematical models

3.1 Basic assumptions

For the performance analysis of the SOFC/MGT hybrid power system, it is necessary to develop mathematical models that govern heat and mass transfer characteristics of each component of the system. For this purpose, some basic assumptions are made as follows:

(1) Supplied fuel to the system is methane (CH_4).
(2) Supplied air to the system is composed of 78.22% of nitrogen (N_2), 20.74% of oxygen (O_2), 0.03% of carbon dioxide (CO_2) and 1.01% of water (H_2O).
(3) All chemical components of working fluids are treated as ideal gases.
(4) Reforming processes in pre-reformer and IIR are steam reforming reactions.
(5) Electrochemical reactions for both hydrogen (H_2) and carbon monoxide (CO) occur at the wall of each tubular SOFC.
(6) Operating cell voltage in each tubular SOFC is constant.

3.2 Quasi-2D model for IIR-SOFC system

Inside the SOFC stacks, fuel stream flows in longitudinal direction along the outer surface, *i.e.* anode, of each tubular SOFC. Air is supplied into the air feed tube located in each tubular SOFC and flows also in longitudinal direction through the annulus between outside of the air feed tube and the inner surface, *i.e*. cathode, of each tubular SOFC. On the other hand, heat is transferred not only through longitudinal direction but also through the direction perpendicular to flow streams. A quasi-2D model is named in this study as a model for mass and heat transfer analyses mainly in flow direction taking into account of heat transfer in its perpendicular direction. Using this model, flow streams in the SOFC are divided into multiple segments as shown in Fig. 2. Each segment is composed of control volumes separated by walls between various flow streams. Chemical compositions and temperature at the exit of the control volume can be computed based on mass and heat balances in each control volume. Chemical reaction processes, such as reforming and electrochemical reactions, contribute to the generation and/or sink of chemical components in each control volume.

Parts of heat generated by electrochemical reactions in tubular SOFC stacks are consumed by direct reforming process occurring simultaneously with electrochemical reactions in the anode, and some part of it is transferred to the IIR. For the heat transfer analysis in flow channels including feed plate and reformer wall, conduction in solid walls, convection in flow channels and radiation among various heat sources must be taken into account.

Energy balance equations governing heat transfer characteristics of control volume in each segment of the quasi-2D model are described as follows:

Inside air feed tube:

$$\sum \dot{n}_{x,i}\bar{h}_x(T_{a,ft,i}) - \sum \dot{n}_{x,i+1}\bar{h}_x(T_{a,ft,i+1}) = h_{a1}A_{ft}(T_{ft,i} - T_{a,ft,m}) \quad (1)$$

where the right-hand side is the heat transfer rate between inner wall of the air feed tube and air flow stream. $\dot{n}_{x,i}$ is the molar flow rate of *x* species at *i*-th segment.

Between air feed tube and inner wall of tubular SOFC:

$$\begin{aligned}&\sum \dot{n}_{x,i+1}\bar{h}_x(T_{a,c,i+1}) - \sum \dot{n}_{x,i}\bar{h}_x(T_{a,c,i}) \\ &= h_{a2}A_c(T_{c,i} - T_{a,c,m}) + h_{a3}A_{ft}(T_{ft,i} - T_{a,c,m}) - \dot{Q}_{elec,ox}\end{aligned} \quad (2)$$

with

$$\dot{Q}_{elec,ox} = \frac{1}{2}\left(z_{\mathrm{H_2}} + z_{\mathrm{CO}}\right)\bar{h}_{\mathrm{O_2}}(T_{a,c,m}) \quad (3)$$

representing the heat transfer caused by the migration of oxygen from the cathode channel to tri-layer (cathode). The first two terms of the right hand side in Eq. (2) represent convective heat transfer rates between air flow stream inside annulus and tube walls (SOFC tube and air feed tube, respectively).

In the solid wall of air feed tube:

$$h_{a1}A_c(T_{ft,i} - T_{a,ft,m}) + h_{a3}A_{ft}(T_{ft,i} - T_{a,c,m}) = 0 \quad (4)$$

For simplicity, the convective heat transfer is only considered in the wall of the air feed tube.

Between outer wall of tubular SOFC and reformer wall:

$$\begin{aligned}&\sum \dot{n}_{x,i+1}\bar{h}_x(T_{f,c,i+1}) - \sum \dot{n}_{x,i}\bar{h}_x(T_{f,c,i}) \\ &= h_{f1}A_c(T_{c,i} - T_{f,c,m}) + h_{f2}A_{rw}(T_{rw,i} - T_{f,c,m}) - \dot{Q}_{elec,fuel}\end{aligned} \quad (5)$$

with

$$\begin{aligned}\dot{Q}_{elec,fuel} = {} & z_{\mathrm{H_2}}\left[\bar{h}_{\mathrm{H_2}}(T_{f,c,m}) - \bar{h}_{\mathrm{H_2O}}(T_{c,i})\right] \\ & + z_{\mathrm{CO}}\left[\bar{h}_{\mathrm{CO}}(T_{f,c,m}) - \bar{h}_{\mathrm{CO_2}}(T_{c,i})\right]\end{aligned} \quad (6)$$

representing the heat transfer caused by the migration of hydrogen and carbon monoxide from the anode channel to tri-layer (anode), and by the migration of steam and carbon dioxide from the tri-layer to the anode channel.

Inside tri-layer solid wall of tubular SOFC:

$$\begin{aligned}&\dot{Q}_{elec,fuel} + \dot{Q}_{elec,ox} - \dot{W}_{FC,i} \\ &= h_{a2}A_c(T_{c,i} - T_{a,c,m}) + h_{f1}A_c(T_{c,i} - T_{f,c,m}) \\ &+ \dot{Q}_{rad} - k_{s,c}A_{s,c}\Delta x\frac{d^2T_c}{dx^2}\end{aligned} \quad (7)$$

with

$$\dot{Q}_{rad} = \sigma A_{rad}\sum_{j=1}^{N}\frac{\left(T_{c,i}^4 - T_{rw,j}^4\right)}{\frac{1-\varepsilon_c}{\varepsilon_c} + \frac{1}{F_{i-j}} + \frac{1-\varepsilon_{rw}}{\varepsilon_{rw}}} \quad (8)$$

representing the radiative heat transfer rate between *i*-th segment of the SOFC wall and all segments of the reformer wall. The last term of the right hand side in Eq. (7) represents the conductive heat transfer rate inside tri-layer solid wall of the SOFC along longitudinal direction.

Between fuel feed plates:

$$\begin{aligned}&\sum \dot{n}_{x,i+1}\bar{h}(T_{f,fp,i+1}) - \sum \dot{n}_{x,i}\bar{h}(T_{f,fp,i}) \\ &= h_{fp}A_{fp}(T_{fp,i} - T_{f,fp,m})\end{aligned} \quad (9)$$

where the right hand side is the convective heat transfer

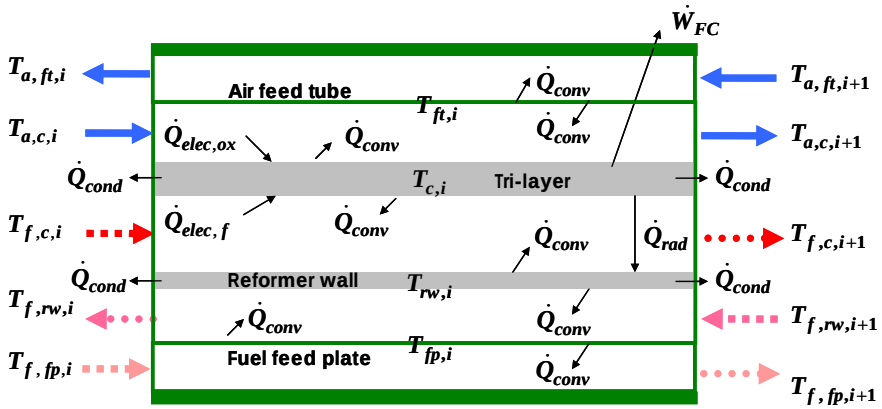

Fig. 3 Schematic diagram of energy flows in a segment of the quasi-2D model in the IIR-SOFC

rate between fuel stream and fuel feed plates.

Between fuel feed plate and reforming wall:

$$\sum \dot{n}_{x,i}\bar{h}_x(T_{f,rw,i}) - \sum \dot{n}_{x,i+1}\bar{h}_x(T_{f,rw,i+1}) = h_{r1}A_{rw}(T_{rw,i} - T_{f,rw,m}) + h_{r2}A_{fp}(T_{fp,i} - T_{f,rw,m}) \quad (10)$$

where, two terms in the right hand side represent convective heat transfer rates between fuel stream and surrounding walls.

Inside fuel feed plate:

$$h_{r2}A_{fp}(T_{fp,i} - T_{f,rw,m}) + h_{fp}A_{fp}(T_{fp,i} - T_{f,fp,m}) = 0 \quad (11)$$

For simplicity, the convective heat transfer is only considered in the wall of fuel feed plate.

Inside reforming wall:

$$\dot{Q}_{rad} = h_{f2}A_{rw}(T_{rw,i} - T_{f,c,m}) + h_{r1}A_{rw}(T_{rw,i} - T_{f,rw,m}) - k_{s,rw}A_{s,rw}\Delta x\frac{d^2T_{rw}}{dx^2} \quad (12)$$

with

$$\dot{Q}_{rad} = \sigma A_{rad}\sum_{j=1}^{N}\frac{\left(T_{c,j}^4 - T_{rw,i}^4\right)}{\frac{1-\varepsilon_c}{\varepsilon_c} + \frac{1}{F_{i-j}} + \frac{1-\varepsilon_{rw}}{\varepsilon_{rw}}} \quad (13)$$

representing the radiative heat transfer rate between *i*-th segment of the reformer wall and all segments of the SOFC wall. The last term of the right hand side in Eq. (12) represents conductive heat transfer rate inside the reformer wall along longitudinal direction.

The heat transfer characteristics in a segment of quasi-2D model in the IIR-SOFC are summarized in Fig. 3.

3.3 Lumped model for the MGT system

Micro gas turbine (MGT) adopted for the SOFC/MGT hybrid power system is composed of four major components; compressor, combustor, turbine and recuperator. Since compressor and turbine in the MGT are generally single stage centrifugal and radial types, respectively, it is good enough to handle them with lumped models. By considering energy balances in compressor and turbine with known inlet conditions, their exit conditions can be simply represented by functions of isentropic efficiencies. In the present study, it is assumed that the turbine inlet temperature (TIT) of the MGT is fixed during any operating conditions.

3.4 System performance

With the definition of current density as the rate of electron transfer per unit activation area of the fuel cell, the electric power produced by the fuel cell can be expressed as follows:

$$\dot{W}_{FC} = V_c jA \quad (14)$$

$$j = 2(z_{H_2} + z_{CO})F/A \quad (15)$$

where, z_{H2} and z_{CO} represent the molar flow rate of electrochemical reactions of hydrogen and carbon monoxide, respectively.

Cell voltage is the difference between the open circuit voltage and voltage losses due to irreversibilities in the fuel cell:

$$V_c = V_{oc} - \Delta V_{loss} \quad (16)$$

where, ΔV_{loss} is the sum of voltage losses due to irreversibilities in the fuel cell. Irreversibilities in the fuel cell include activation polarization, ohmic losses, concentration loss, etc. At the high operating temperature of the SOFC, diffusion is a very efficient process, and thus the concentration loss is ignored [4]. In the present study, activation polarization and ohmic losses are only taken into considerations as below:

$$\Delta V_{loss} = \Delta V_{act} + \Delta V_{ohm} \quad (17)$$

where ΔV_{act} is the activation polarization, and ΔV_{ohm} is the ohmic losses.

Activation polarization is caused by the slowness of the electrochemical reactions taking place on the surface of electrodes, which is very nonlinear and difficult to be

expressed analytically. The model for activation polarization used in this study is adopted from Achenbach [10]:

$$\Delta V_{act} = \Delta V_{act,a} + \Delta V_{act,c} = jr_c + j_{\mathrm{H}_2} r_{a,\mathrm{H}_2} \tag{18}$$

with

$$\frac{1}{r_c} = \frac{4F}{RT} k_c \left(\frac{p_{\mathrm{O}_2}}{P_0} \right)^m \exp\left(-\frac{E_c}{RT} \right) \tag{19}$$

$$\frac{1}{r_{a,\mathrm{H}_2}} = \frac{2F}{RT} k_{a,\mathrm{H}_2} \left(\frac{p_{\mathrm{H}_2}}{P_0} \right)^m \exp\left(\frac{-E_a}{RT} \right) \tag{20}$$

where, r represents the area specific electrical resistance. The influence of the partial pressure on the losses is accounted by the slope of m=0.25. Each activation energy of the cathode and anode is set to E_c = 160kJ/mol and E_a = 110kJ/mol. And, the pre-exponential factors are given as $k_c = 1.49 \times 10^{10}$, $k_{a,\mathrm{H2}} = 2.13 \times 10^8 \mathrm{A/m^2}$.

Ohmic losses occur due to the electrical resistance to the flow of electrons or ionic species. Figure 4 shows paths of the electron through the cathode, the oxygen ion through the electrolyte, and the electron through the anode in a tubular SOFC. In this study, an ohmic loss model taking into account of realistic electron/ion paths is developed based on Tanaka *et al.* [11]. In Fig. 4, angle $A\pi$ and $B\pi$ are related to the extent of electrical contact on the half of the cell tube and the interconnector, respectively. The final forms of ohmic losses in a tubular SOFC are represented as follows; anode, cathode, electrolyte, and interconnector.

$$\Delta V_{ohm,a} = \frac{\rho_a j (A\pi D)^2}{8 d_a} \tag{22}$$

$$\Delta V_{ohm,c} = \frac{\rho_c j A (\pi D)^2}{8 d_c} \left[A + 2(1 - A - B) \right] \tag{23}$$

$$\Delta V_{ohm,e} = j \rho_e d_e \tag{24}$$

$$\Delta V_{ohm,int} = j (A\pi D) \rho_{int} \frac{d_{int}}{w_{int}} \tag{25}$$

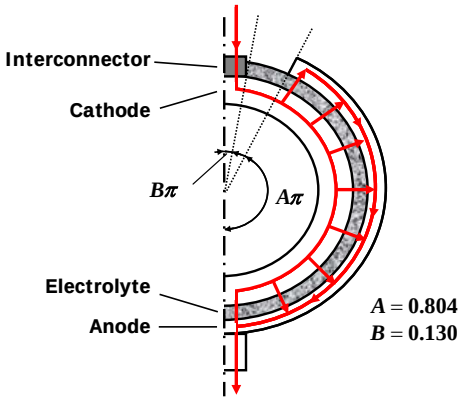

Fig. 4 A model for the calculation of ohmic losses in a tubular SOFC

where ρ_i , d_i, and D are the resistivity and thickness of component i, and the mean diameter of a tubular SOFC, respectively. w_{int} is the width of the interconnector. Resistivity of each layer of SOFC is treated to be a function of the local operating temperature [12].

4. Results and discussions

Figure 5 show the influence of operating temperature and pressure on the tubular SOFC. The decrease of operating cell voltage with high current density is caused by the proportionality of voltage losses to current density. These figures also show that mathematical models used in this study reasonably predict the experimental data measured by Singhal [13,14]. However, due to the underprediction at low temperature, the electrochemical model used in this study should be modified if applied to the intermediate temperature SOFC whose operating temperature is about 600~800°C.

Number of segments in the quasi-2D model influences the performance analysis as indicated in Table 1. As number of segments in the quasi-2D model is increased, predicted results approach to the data released by Sie-

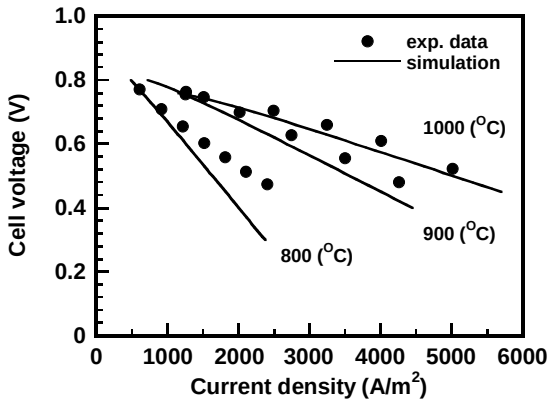

(a) Temperature (data from Singhal [13])

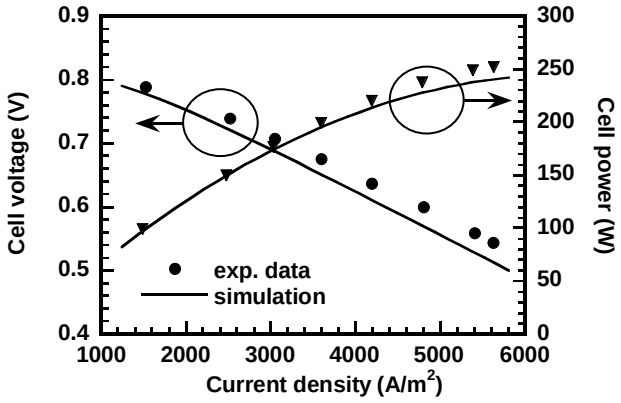

(b) Pressure (3atm) (data from Singhal [14])

Fig. 5 Influence of temperature and pressure on tubular SOFC performance

Table 1 Influence of number of segments in a quasi-2D model on the performance of the SOFC/MGT hybrid power system

Parameter	Siemens-Westinghouse [6]	Number of segments			
		N=1	N=5	N=10	N=20
Current density, A/m^2	3200	**3200**	**3200**	**3200**	**3200**
Operating cell voltage, V_c	0.610	0.540	0.607	0.611	0.613
Pressure ratio	2.9	**2.9**	**2.9**	**2.9**	**2.9**
Air flow rate, kg/s	0.5897	0.7128	0.5964	0.5898	0.5867
TIT, ^oC	840	**840**	**840**	**840**	**840**
SOFC DC power, kW	187	175.0	184.3	184.7	185.0
SOFC AC power, kW	176	166.4	175.0	175.5	175.7
GT AC power, kW	47	55.4	46.7	46.2	45.9
Net AC power, kW	220	**220**	**220**	**220**	**220**
System efficiency, %	57	56.0	59.8	60.1	60.2
Cell active area, m^2	96	101.3	94.9	94.5	94.3

Bold characters are given values.

mens-Westinghouse [6]. Also, it is clearly shown that the lumped model analysis under- or over-estimates the performance data. It is proven that the quasi-2D model can predict the performance of the SOFC/MGT hybrid power system more accurately than lumped model, and its accuracy can be improved with increased number of segments.

5. Conclusions

In this study, more reliable design point performance of the tubular SOFC/MGT hybrid can be obtained by using the developed quasi-2D model. Detailed heat and mass transfer with reforming and electrochemical reactions in the SOFC are mathematically modeled. Special attention is paid to the ohmic losses in tubular SOFC. Results verify that a quasi-2D model is more proper to calculate both the SOFC and SOFC/MGT hybrid system performance in comparison with a lumped model.

As a future plan, effects of different internal constructions of the SOFC system and design parameters such as current density and recirculation ratio on the system performance will be investigate. Also, the quasi-2D model will be adapted to the performance analysis at part-load operating conditions. This model may provide useful information for the phenomena related to the fuel depletion near the end of the tubular SOFC by predicting the amount of local fuel consumptions.

References

(1) Harvey, S. P., and Richter, H. J., 1994, "Gas Turbine Cycles with Solid Oxide Fuel Cells – Part I: Improved Gas Turbine Power Plant Efficiency by Use of Recycled Exhaust Gases and Fuel Cell Technology," *ASME J. of Energy Resources Technology*, Vol.116, pp.305-311.

(2) Campanari, S., 2000, "Full-Load and Part-Load Performance Prediction for Integrated SOFC and Microturbine Systems," *ASME J. of Engineering for Gas Turbines and Power*, Vol.122, pp.239-246.

(3) Freni, S., Aquino, M., and Passalacqua, E., 1994,"Molten Carbonate Fuel Cell with Indirect Internal Reforming," *J. of Power Sources*, Vol.52, pp.41-47.

(4) Massardo, A. F., and Lubelli, F., 2000, "Internal Reforming Solid Oxide Fuel Cell-Gas Turbine Combined Cycles (IRSOFC-GT) Part A : Cell Model and Cycle Thermodynamic Analysis," *ASME J. of Engineering for Gas Turbines and Power*, Vol.122, pp.27-35.

(5) Veyo, S. E., Shockling, L. A., Dederer, J. T., Gillett, J. E., and Lundberg, W. L., 2002, "Tubular Solid Oxide Fuel Cell/Gas Turbine Hybrid Cycle Power Systems: Status," *ASME J. of Engineering for Gas Turbines and Power*, Vol.124, pp. 845-849.

(6) George, R. A., 2000, "Status of Tubular SOFC Field Unit Demonstrations," *J. of Power Sources*, **86**, pp.134~139.

(7) Kim, J. H., and Suzuki, K., 2001, "Performance Analysis of SOFC/MGT Hybrid System," *Proceedings of the KSME Spring Annual Meeting B*, pp.703-707.

(8) Bevc, F., 1997, "Advances in Solid Oxide Fuel Cells and Integrated Power Plants," *Instn Mech. Engrs, Part A, Inter. J. of Power and Energy*, **211**, pp.359-366.

(9) George, R. A., and Bessette, N. F., 1998, "Reducing the Manufacturing Cost of Tubular SOFC Technology," *J. of Power Sources*, **86**, pp.131-137.

(10) Achenbach, E., 1994, "Three-Dimensional and Time-Dependent Simulation of a Planar Solid Oxide Fuel Cell Stack," *J. of Power Sources*, **49**, pp.333-348.

(11) Tanaka, K., Wen, C. and Yamada, K., 2000, "Design and Evaluation of Combined Cycle System with Solid Oxide Fuel Cell and Gas Turbine," *Fuel*, **79**, pp.1493-1507.

(12) Bessette II, N. F. and Wepfer, W. J., 1995, "A Mathematical Model of a Tubular Solid Oxide Fuel Cell," *J. of Energy Resources Technology*, **117**, pp.43-49.

(13) Singhal, S. C., 1997, "Progress in Tubular Solid Oxide Fuel Cell Technology," Electrochemical Society Proceedings, Vol.99-19, pp.39~51.

(14) Singhal, S. C., 2000, "Advances in Solid Oxide Fuel Cell Technology," *Solid State Ionics*, **135**, pp.305~313.